Computations of Hypersonic Flow of a Diatomic Gas in Rotational Non-Equilibrium past 3D Blunt Bodies Using the Generalized Boltzmann Equation

Christopher D. Wilson[a], Ramesh K. Agarwal[a], and Felix G. Tcheremissine[b]

[a]*Department of Mechanical Engineering and Materials Science*
Washington University in St. Louis, Missouri 63130, USA

[b]*Mechanics Department*
Computing Center of Academy of Science, Moscow, Russia

Abstract. Direct methods for solving the generalized Boltzmann equation are advanced by simulating flow past three-dimensional immersed bodies in diatomic nitrogen in rotational-translational non-equilibrium. The simulations are performed by solving the entire domain with the generalized Boltzmann equation using a solver based upon the conservative discrete ordinates method of Tcheremissine. Coarse and refined grid solutions are generated for three axisymmetric three-dimensional bodies – blunt body, bicone, and hollow flared cylinder. The solutions are compared and a parallel implementation is developed to enable further levels of grid refinement.

Keywords: Boltzmann Equation, 3D, Compressible Flow, Hypersonic Flow, Rotational Non-Equilibrium
PACS: 51.10.+y, 05.20.Dd

INTRODUCTION

Direct finite-difference methods for solving the Boltzmann equation have only recently seen significant advancements. As a result, direct solution methods for the Boltzmann equation have not advanced to the same level as their statistical or continuum counterparts. This paper focuses on further advancing the state of the art of direct methods by developing the capabilities for solving flow around 3D immersed bodies in non-equilibrium hypersonic flows with increasing levels of grid refinement. The advancements discussed in this paper include a parallelization scheme for the baseline mono-molecular model of Tcheremissine [1], computation of baseline coarse grid solutions for several immersed bodies (axisymmetric blunt body, bicone, and hollow-flared-cylinder), and computations of solutions with a higher level of grid refinement on a parallel computing platform and comparisons of fine grid solutions with coarse grid solutions for hypersonic rarefied flow past an axisymmetric body bathed in nitrogen with rotational-translation (RT) non-equilibrium.

DEVELOPMENT AND PARALLEL IMPLEMENTATION

In order to enhance the capabilities of the three-dimensional classical Boltzmann solver based on Tcheremissine's method [1], by including capabilities for increasing levels of grid refinement to improve solution accuracy and the inclusion of additional internal degrees of freedom (rotational and vibrational), and the capability for simulating mixtures of gases, the parallelization of the three-dimensional solver was found to be a must needed enhancement and extension. A parallelization scheme was developed for this purpose and implemented.

Modifications to the Baseline 3D Generalized Boltzmann Solver

Tcheremissine's code was originally written to simulate a jet issuing into a vacuum. The code was modified to allow for the simulation of flow around immersed bodies. The grid definition was modified to define the immersed body geometry. The code employs a Cartesian grid whereby grid points are defined by three separate distributions along the X/λ, Y/λ, and Z/λ axes. As a result, resolving the surface of a curvilinear body requires a significant number of grid points. These extra grid points used to resolve the surface of the body also result in the generation of superfluous nodes near the farfield boundaries of the domain, with corresponding cells of excessively high aspect ratios. These consequences result in a significant increase in the memory required to execute a solution. Similar challenges are encountered when attempting to resolve the boundary layer near the surface of the body.

Simulations were performed at Mach 3 and Mach 7 for several immersed body geometries. In order to enable higher Mach number simulations, it is necessary to increase the expanse of the velocity space domain such that the majority of the distribution function is contained within the domain. Increase in the expanse of the velocity space domain results in greater memory requirement in the physical space, which precluded running fine grid solutions for the hollow-flared-cylinder on the available computing hardware.

Code Parallelization

Based upon the results obtained after modifying the baseline code to simulate flow around immersed bodies, it became necessary to parallelize the code to enable higher levels of grid refinement. The memory requirements for a conventional continuum solver are primarily dependent upon the physical space grid dimensions. For direct numerical simulation of the Boltzmann equation, the physical space grid size is only one of the key contributing factors for determining the memory requirement and the corresponding computation time; the other key contributing factor is the velocity space grid refinement. The total number of grid points required for a physical space Cartesian grid is equal to the product of the number of grid points in each physical space coordinate direction, $N_x N_y N_z$. The total number of grid points in velocity space, also assuming a Cartesian grid, is equal to the product of the number of grid points in each coordinate velocity direction, $N_u N_v N_w$. As a result, the total number of grid points for a direct numerical simulation of the Boltzmann equation is the product of the total number of grid points in physical space and the total number of grid points in velocity space, $N_x N_y N_z N_u N_v N_w$. If additional degrees of freedom are considered (i.e. rotational and vibrational), and more than one gas specie is included, the total number of grid points required to define the distribution function increases by the product of the number of rotational energy levels, the number of vibrational energy levels, and the number of species, $N_{Rot} N_{Vib} N_{Spe}$. Therefore, the total expanse of the distribution function is the product of the total number of grid points, the total number of energy levels, and the total number of species, $N_x N_y N_z N_u N_v N_w N_{Rot} N_{Vib} N_{Spe}$. A problem that requires only 5000 grid points in physical space could require more than 550 million elements to define the distribution function. Furthermor, over five gigabytes of physical memory is required to store the distribution function for these 550 million elements.

A three-dimensional physical space defined by only 5000 points is extremely coarse by any continuum grid generation standard. Therefore, a hybrid parallelization approach was implemented to facilitate more refined physical space grids in the calculations. The splitting scheme that is used to calculate the distribution function enables parallelization to be implemented in a rather straightforward manner. The relaxation phase of the splitting scheme is independent of neighboring physical space grid points. Therefore, the only portion of the splitting scheme that needs to be parallelized is the free molecular phase. The free molecular phase is only dependent upon the changes in the distribution function in physical space. Thus, the physical space domain can be separated into similarly sized zones and distributed to individual computational nodes on a cluster. The number of computational nodes in the cluster enables a proportionate increase in the number of grid points in physical space. Additionally, multiple cores on a single computational node can be utilized to decrease the computation time.

A hybrid parallelization approach was utilized to parallelize the free molecular phase of the code. OpenMP was utilized to enable multiple cores on a single computational node to simultaneously perform computations on different physical space nodes. OpenMP is an application programming interface (API) specifically targeted at shared-memory system parallel programming. OpenMP is relatively easy to implement, only decreases computation time, and does not enable the increase of the total number of grid point. The Message Passing Interface (MPI) enables developing programs that can capitalize on the benefits of a distributed memory system. MPI is more difficult to implement, but is required for larger grid sizes. MPI was used to enable multiple computational nodes on a computing cluster to solve different zones of the physical space computational domain in parallel. As mentioned previously, both OpenMP and MPI were only applied to the free molecular phase of the Boltzmann solver.

COARSE GRID SOLUTIONS

Three immersed axisymmetric body geometries were used to demonstrate application of the three-dimensional generalized Boltzmann equation (GBE) solver. These geometries include a blunt body, a bicone, and a hollow flared cylinder, shown in Figure 1. Extensive experimental work has been conducted for hypersonic flow of nitrogen past a bicone and a hollow-flared-cylinder [2]. These geometries were chosen to facilitate eventual direct comparison of the Boltzmann solutions with the experimental data. All the geometries are modeled as quarter-bodies, since the incoming flow is at zero degree angle of attack. The X-axis is along the centerline of the body, with reflection about the XY plane at $Z/\lambda = 0$ and the ZX plane at $Y/\lambda = 0$. An inflow boundary condition was imposed in the YZ plane at $X/\lambda = 0$. All the other planar boundaries of the domain were assumed to be outflow boundaries.

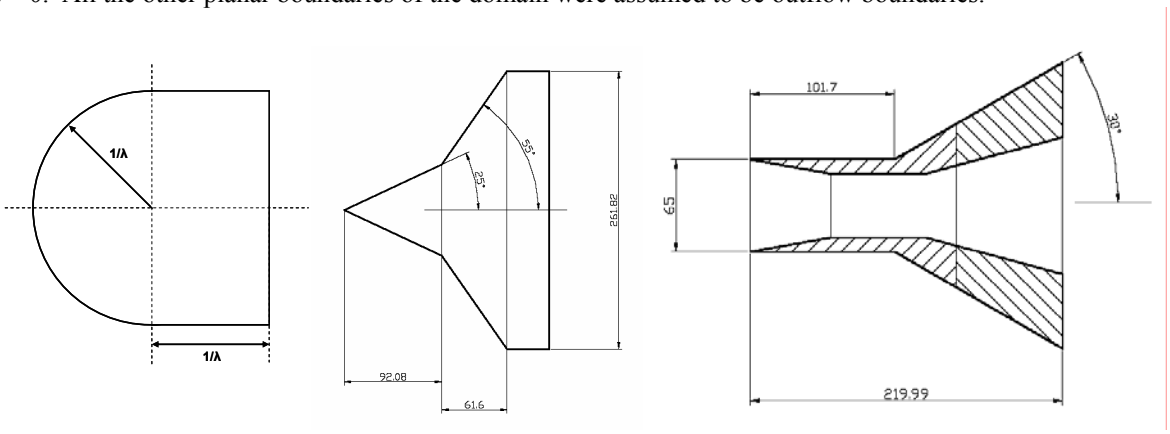

FIGURE 1. Immersed Body Geometries – Blunt Body, Bicone, Hollow Flared Cylinder

The blunt body geometry is adapted from Josyula [3]. Hypersonic flow of nitrogen past a bicone and hollow flared cylinder in rotational-translation non-equilibrium are benchmark test cases for which experimental data is available [4]. The bicone and hollow flared cylinder were adapted from Harvey [2]. Coarse grid solutions for the blunt body and bicone were run at Mach 3 and 7 at three different Knudsen numbers (0.01, 0.1, and 1.0). Coarse grid solutions for the hollow flared cylinder were run at Mach 3 at the same Knudsen numbers. Adequately refined Mach 7 solutions could not be achieved on the available computing hardware due to higher memory requirements imposed by the expanded velocity space grid. The adsorptive wall boundary condition was used at the body surface for all of the geometries. As an example of the solutions, Figures 2 - 5 present three-dimensional isometric views of Mach number and density contours around the blunt body at Mach 3 and Kn = 1. The views show the flow properties in the ZX plane at $Y/\lambda = 0$, the XY plane at $Z/\lambda = 0$, and YZ plane at $X/\lambda = X_{max}$.

By examining the contour plots for each Knudsen number, it is clear that the variation in Knudsen number has a direct impact on the extent of the shock wave upstream of the body. As the Knudsen number increases (i.e. the flow becomes more rarefied) the shock becomes diffuse and extends further upstream of the nose of the body. Additionally, the density variations extend further downstream along the surface of the body past the nose. When Mach number increases from three to seven, the extent of the high density region of the shock wave increases. Additionally, it appears that the shock thickness along the stagnation line becomes slightly smaller. The variations in Knudsen number have the same effect for the Mach 7 solutions as for the Mach 3 solutions. It is interesting to note that the density decreases as the Knudsen number decreases (i.e. the flow tends toward a continuum). This decrease in density can be most likely attributed to the grid density near the surface of the body.

Since the hollow-flared-cylinder has an internal flow path, the contraction ratio needs to be examined to determine whether the contraction ratio between the inlet and the throat will result in over-contraction and a subsequent un-start. The area ratio between the inlet and the throat is approximately 0.48. The contraction ratio, A*/A, that will result in Mach 1 at the throat is 0.24. Therefore, there is plenty of margin between the contraction ratio of the hollow-flared-cylinder and an area ratio that would result in over-contraction. Examining the Kantrowitz self-start limit produces the same observation regarding the contraction ratio. The grid density within the internal flow path can have a direct impact on the behavior of the inlet. Therefore, a higher grid density for the internal flow path needs to be used to ensure an accurate result for the shock structure and the stagnation line properties.

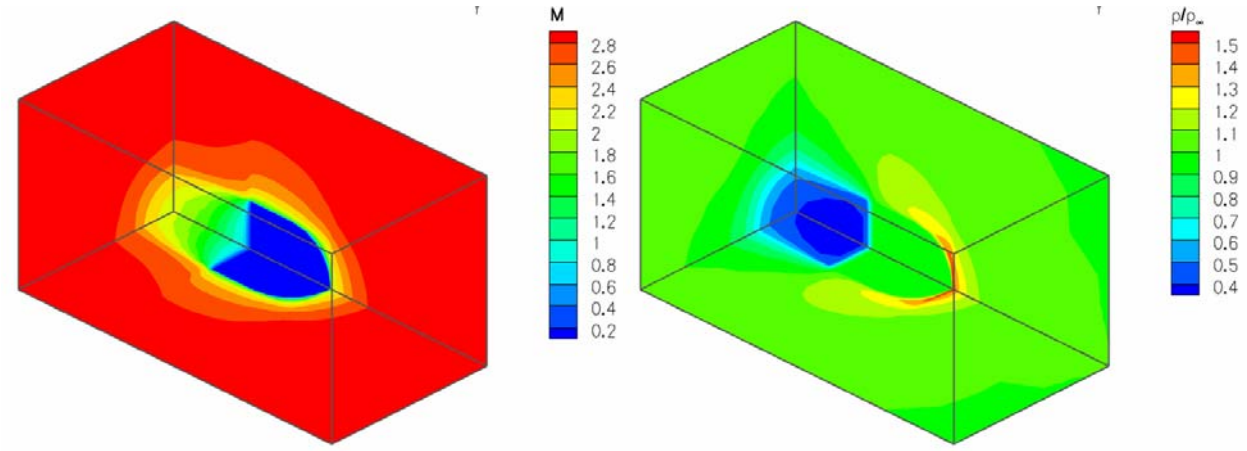

FIGURE 2. Blunt Body: 3D Mach and Density Contours at Mach 3 and Kn = 1

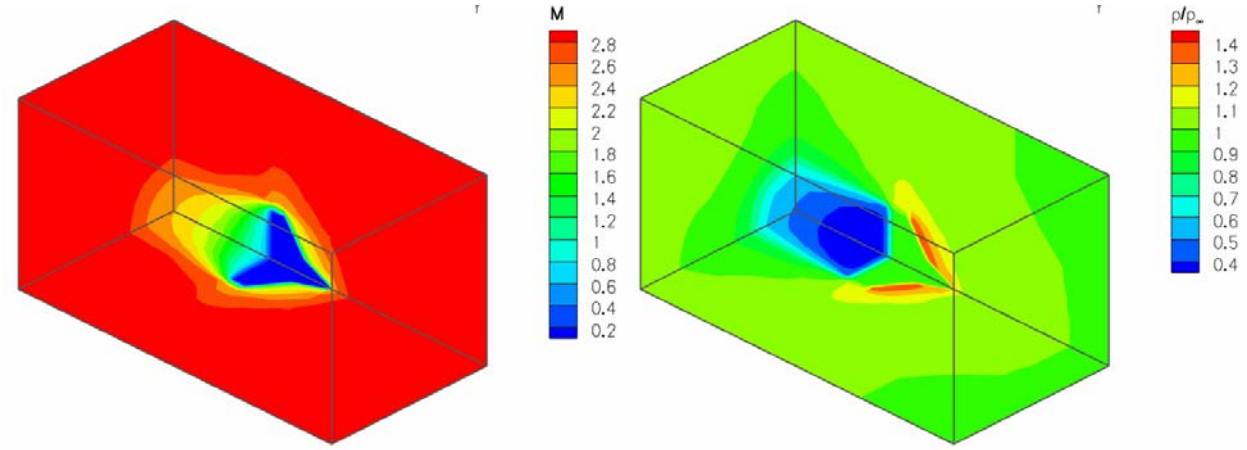

FIGURE 3. Bicone: 3D Mach and Density Contours at Mach 3 and Kn = 1

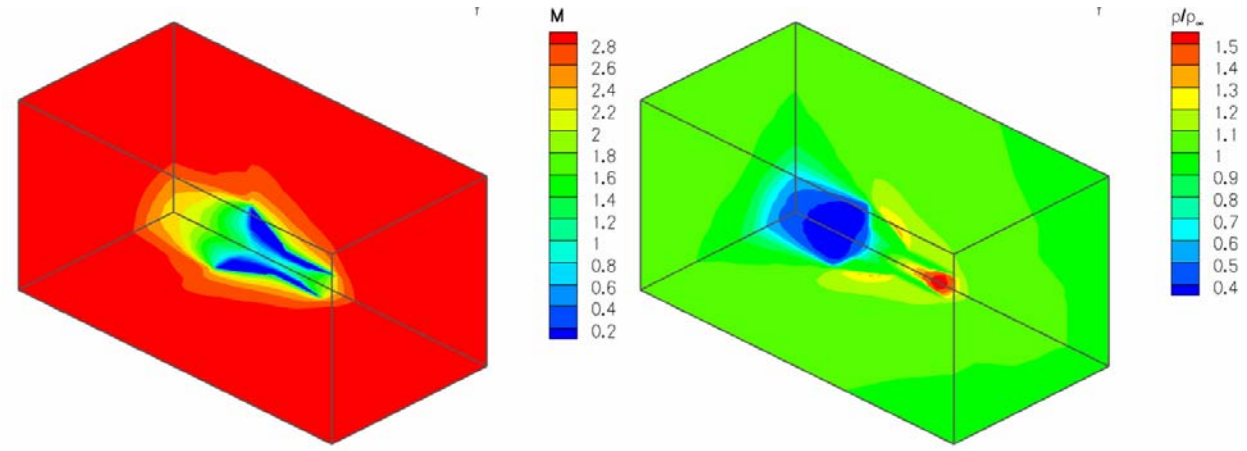

FIGURE 4. Hollow Flared Cylinder: 3D Mach and Density Contours at Mach 3 and Kn = 1

REFINED GRID SOLUTIONS

The grid refinement was performed for the axisymmetric blunt body. The grid point distribution was roughly doubled in each of the coordinate directions. The following sections present the results obtained using the refined grid and comparison of the results obtained with coarse and refined grids.

Flow Past a Blunt Body

The geometry of the blunt body used for the refined grid solution is the same as that presented previously. A refined grid solution is generated at Mach 3 and a Knudsen number of 1.0. The adsorptive wall boundary condition is used for the body surface. Figure 4 presents three-dimensional isometric views of Mach number and density contours around the blunt body.

The results obtained using the refined grid present a much more smoothly defined shock wave upstream of the body. The primary differences are in the gradients of flow properties near the surface. It is clear from both the contours and the stagnation line plots that the shock structure is better defined for the refined grid solutions. The shock wave upstream of the body for the coarse grid solutions was smeared over a longer distance upstream of the body.

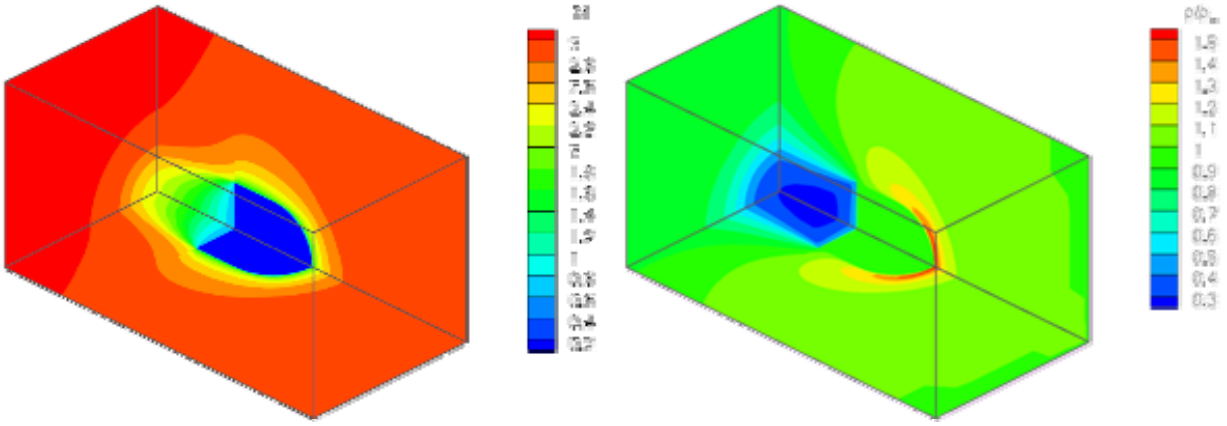

FIGURE 5. Refined Grid Blunt Body: 3D Mach and Density Contours at Mach 3 and Kn = 1

Solution Comparison

A converged solution on the coarse grid was obtained after approximately 1000 iterations and ten hours of run time on a quad-core Intel processor based machine with eight gigabytes of physical memory. A converged solution on the refined grid was obtained after approximately 5000 iterations and 37 days of run time on a dual quad-core Intel processor based machine with 72 gigabytes of physical memory.

It can be seen that there is a difference between the coarse grid solutions and the refined grid solutions by simply comparing the contour plots and the stagnation streamline plots of various flow variables. The stagnation streamline plots clearly show that the flow properties are smeared across a larger distance in the coarse grid solutions. The decrease in shock thickness, and the tendency of the flow properties to approach the stagnation values, with an increase in the grid resolution near the nose of the body is a direct result of increasing the grid refinement upstream of the body. Additionally, the conclusion can be drawn that, at the current levels of grid refinement, the solutions are still grid dependent. Figure 6 demonstrates the impact of grid refinement on Mach number for constant lines of Z/λ between the stagnation streamline and the upper surface of the body.

Additional metrics for evaluating the impact of grid refinement are to examine the interaction of the flow along the surface of the immersed body. To facilitate this evaluation, estimates of proportional values for skin friction, pressure, and heat transfer were calculated along the top surface of the blunt body. Figure 7 presents these values for both the coarse grid and the refined grid solutions. Both skin friction and heat transfer are under predicted by approximately 75% with the coarse grid solutions when compared to the refined grid solutions. The coarse grid solutions also over predict the pressure coefficient by approximately 5%. Additional levels of grid refinement will be required in order to obtain better estimates for these parameters.

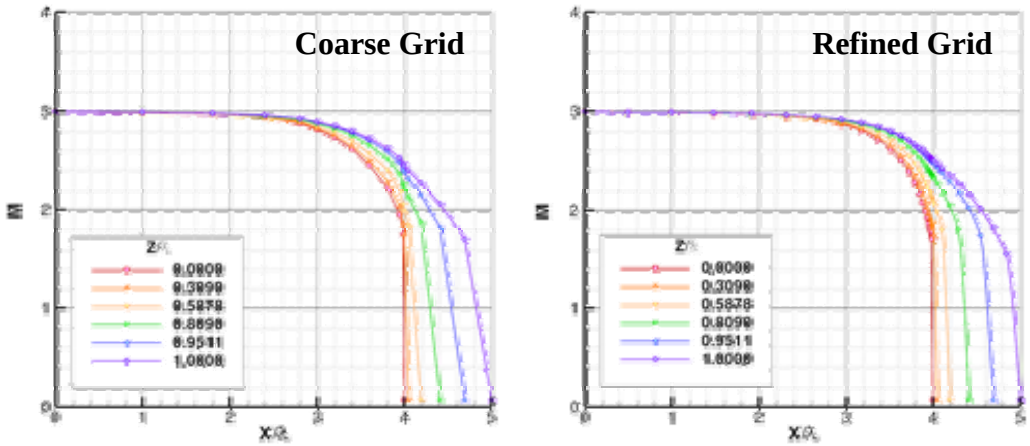

FIGURE 6. Coarse and Refined Grid Solution Comparison of Mach Number at Constant Z/λ

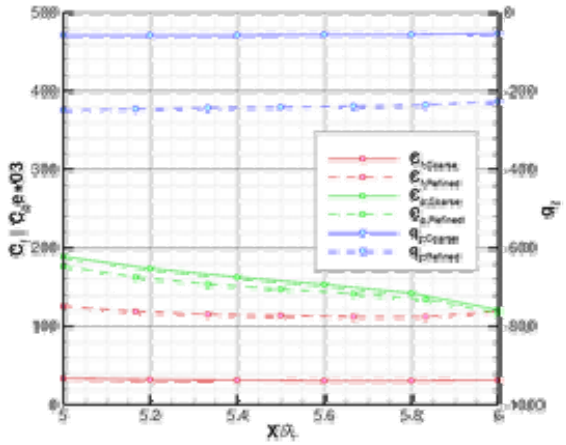

FIGURE 7. Parameters Comparing Fluid/Body Interaction along the Upper Surface of the Blunt Body

SUMMARY

The two main approaches for obtaining more refined, less grid dependent solutions, are to implement a more sophisticated grid generation scheme and to improve the numerical approach used in the relaxation phase of the Boltzmann solver. Since the Boltzmann equation is presented strictly in terms of an orthogonal coordinate system, and is not conformally mapped, local adaptive mesh refinement could be used to improve both resolution of the immersed body surface and of high gradient flow field structures (i.e. shock waves). The current parallelization approach only addresses the free molecular phase. The numerical scheme currently used in the relaxation phase is not well conditioned to take advantage of parallelization. Therefore, a restructuring of the numerical approach used in the relaxation phase could enable that phase of the computation cycle to take advantage of parallelization.

REFERENCES

1. Tcheremissine, Felix G. Solution of the Wang-Chang-Uhlenbeck Master Equation. *Doklady Physics* 47, no. 12: 872-875.
2. Harvey, John K. 2003. A Review of a Validation Exercise on the use of DSMC Method to Compute Viscous/Inviscid Interactions in Hypersonic Flow. In *36th AIAA Thermophysics Conference, Orlando, Florida, 23-26 June 2003,* AIAA Paper 2003-3643. Washington DC: AIAA.
3. Josyula, Eswar. 2000. Computational Study of Vibrationally Relaxing Gas Past Blunt Body in Hypersonic Flows. *Journal of Thermophysics and Heat Transfer* 14, no. 1 (January-March): 18-26.
4. Holden, Michael S., Graham V. Candler, and John K. Harvey. 2003. Measurements in Regions of Low Density Laminar Shock Wave/Boundary Layer Interaction in Hypervelocity Flows and Comparison with Navier-Stokes Predictions. In *41st Aerospace Sciences Meeting and Exhibit, Reno, Nevada, 6-9 January 2003,* AIAA Paper 2003-1131. Washington DC: AIAA.